

Benchmarking Differentially Private Residual Networks for Medical Imagery

Sahib Singh ^{*1 2} Harshvardhan D. Sikka ^{*1 2 3} Sasikanth Kotti ^{1 4} Andrew Trask ^{1 5}

Abstract

Hospitals and other medical institutions often have vast amounts of medical data which can provide significant value when utilized to advance research. However, this data is often sensitive in nature and as such is not readily available for use in a research setting, often due to privacy concerns. In this paper, we measure the performance of a deep neural network on differentially private image datasets pertaining to Pneumonia. We analyze the trade-off between the models accuracy and the scale of perturbation among the images. Knowing how the models accuracy varies among different perturbation levels in differentially private medical images can be quite a useful measure for hospitals to know. Furthermore, we also seek to measure the usefulness of local differential privacy for such medical imagery tasks and see if there's room for improvement.

Introduction

Pneumonia is an infection that causes inflammation in the alveoli of the lungs, and can be caused by numerous infectious agents. Often pneumonia is the resulting complication of an existing infection. Infectious agents include Coronaviruses, like SARS-CoV2, Influenza Viruses, and various bacterial species (Howley, 2020). According to the Centers for Disease Control and Prevention, there are about 250,000 hospitalization and about 50,000 deaths every year owing to pneumonia (Howley, 2020). Patient condition and immune response to pneumonia can vary based on the specific conditions and factors involved in the patient's own health and physiology, as well as the characteristics of the infectious agent (Howley, 2020). Key contributing factors include:

^{*}Equal contribution ¹OpenMined ²Manifold Computing Group ³Harvard University ⁴Indian Institute of Technology Jodhpur ⁵University of Oxford. Correspondence to: Sahib Singh <sahibsin@alumni.cmu.edu>, Harshvardhan D. Sikka <has727@g.harvard.edu>, Andrew Trask <andrew@openmined.org>.

- Pre-existing comorbidities and general state of overall health in the infected individual
- Virulence level of the infectious organism.
- The level of exposure to the infectious agent. Increased proximity leads to significantly larger risk of infection severity, along with chance of infection. This is due to the increased inhalation of the infectious agent through various mediums. (Howley, 2020)

The percentage of deaths attributed to pneumonia and influenza is 8.2% in the United States, exceeding the threshold of epidemic classification, which is 7.2% (cdc, 2020). Recently, deaths due to pneumonia have sharply increased due to the worldwide presence of COVID-19 and the SARS-CoV2 virus. The rapid construction and evaluation of relevant models to track, diagnose, or support the treatment and mitigation of the COVID-19 is critical given global circumstances. Given the urgent need for these developments and the inherently sensitive nature of medical data, training and evaluating models while maintaining obfuscation of critical personal information in the data corpus is vital.

The field of Differential Privacy approaches these constraints through various methods, including the direct obfuscation of data (Dwork et al., 2006a;b). In this work, we analyze the impact of differentially private datasets on the performance of a popular image classification model, Resnet (He et al., 2016; Szegedy et al., 2017). We compare the model performance on the Chest X-Ray Dataset (Kermany et al., 2018) with different levels of Perturbation while ensuring the images are differentially private. This analysis aims to aid medical professionals better understand the tradeoff between accuracy and data privacy, and may serve as a useful reference to better evaluate how sensitive information must be preserved while still ensuring the data remains useful for research purposes.

This text is organized as follows: We start off by talking about the related research previously conducted in the DP space, followed by an introduction to the DP mechanisms as they pertain to the our findings. We then evaluate the relevant experiments conducted. Finally, we discuss the significance of these findings and the potential future direc-

tions.

Related Work

It's worth noting that there are several techniques to achieve Differential Privacy for images. The DP technique used in this experiment is called Local Differential Privacy which adds perturbations directly to the image. Another state of the art technique for achieving DP in a similar setting is by adding noise during the model training process. Techniques such as DP-Stochastic Gradient Descent (DP-SGD) can be used for such purposes. DP-SGD (Abadi et al., 2016) is a modification of the stochastic gradient descent algorithm which provides provable privacy guarantees. It is different from the standard SGD algorithm since it bounds the sensitivity of each gradient and provides moments accountant to keep track of it's privacy loss.

Lately, there has also been research in applying Differential Privacy during the test-time inference stage of Deep Learning. These include mechanisms such Cloak (Mirshghallah et al., 2020) and ARDEN (Wang et al., 2018). There are also well understood cryptographic protocols such as Homomorphic Encryption (HE) and Secure Multi-Party Computation (SMC) which could be used to encrypt data during training and inference phases. However the computational costs associated with these cryptographic techniques could be prohibitively expensive. A comprehensive list of such privacy preserving techniques can be found in Mirshghallah et al. (2020).

We would additionally like to acknowledge similar work which was done earlier in a more theoretical setting (Fan, 2019). Our paper builds upon the work and applies it towards the Health-care domain, and is relevant in Medical Research in particular.

Preliminaries

In this section we discuss the fundamental privacy preserving concepts used throughout the paper.

Differential Privacy (DP). (Dwork et al., 2006a;b)

The central idea in differential privacy is the introduction of randomized noise to ensure privacy through plausible deniability. Based on this idea, for $\epsilon \geq 0$, an algorithm A is understood to satisfy Differential Privacy if and only if for any pair of datasets that differ in only one element, the following statement holds true.

$$P[A(D) = t] \leq e^\epsilon P[A(D') = t] \quad \forall t$$

Where D and D' are differing datasets by at most one element, and $P[A(D) = t]$ denotes the probability that t is the output by A . This setting approximates the effect of

individual opt-outs by minimizing the inclusion effect of an individuals data.

However, one major limitation of this kind of Differential Privacy is that the data owners will have to trust a central authority, i.e. the database maintainer, to ensure their privacy. Hence in order to ensure stronger privacy guarantee we utilize the concept of Local Differential Privacy (LDP) (Bebensee, 2019). We say that an algorithm π satisfies ϵ -Local Differential Privacy where $\epsilon > 0$ if and only if for any input v and v' .

$$\forall y \in Range(\pi) : P[\pi(v) = y] \leq e^\epsilon P[\pi(v') = y]$$

For $\epsilon = LDP$ the privacy loss is captured by ϵ . Having $\epsilon = 0$ ensures perfect privacy as $e^{(0)} = 1$, on the other hand, $\epsilon = \infty$ provides no privacy guarantee. The choice of ϵ is quite important as the increase in privacy risks is proportional to e^ϵ .

Laplace Distribution. (Dwork et al., 2014)

The Laplace distribution, also known as the double-exponential distribution, is a symmetric version of the exponential distribution. The distribution centered at 0 (i.e. $\mu = 0$) with scale β has the following probability density function:

$$Lap(x|b) = \frac{1}{2\beta} \exp\left(\frac{-|x|}{\beta}\right)$$

The variance of this distribution is $\sigma^2 = 2\beta^2$.

Laplace Mechanism. (Dwork et al., 2006b; 2014)

Laplace Mechanism independently perturbs each coordinate of the output with Laplace noise (from the Laplace distribution having mean zero) scaled to the sensitivity of the function.

Given $\epsilon \geq 0$ and a target function f , the Laplace Mechanism is the randomizing algorithm

$$A_f(D) = f(D) + x$$

where x is random variable drawn from a Laplace distribution, corresponding to perturbation. Δf corresponds to the global sensitivity of function f , defined as over all dataset pairs that differ in only one element (D, D') .

Experimental Result

The experiments discussed in this section used an 18-Layer Residual Network (ResNet) previously trained to achieve convergence on the ImageNet task. ResNets share many ideas with the popular VGG architecture (Simonyan & Zisserman, 2014; Szegedy et al., 2017), with significantly fewer filters and overall decreased complexity. They make use of

Table 1. Accuracy % vs Perturbation Scale

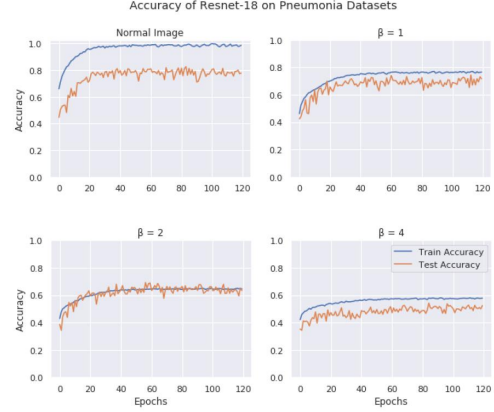
Accuracy	Original	$\beta = 1$	2	4
Test	82.69%	74.35%	69.23%	54.16%
Train	99.98%	77.11%	65.08%	58.03%

identity connections between sets of layers as a solution to the common problem of gradient signals vanishing during backpropagation in very deep networks (He et al., 2016). The experimental setup consisted of training the selected model on an image classification task consisting of the Chest X-Ray dataset (Kermany et al., 2018). The Chest X-Ray dataset consists of approximately 5,800 images sourced from chest radiography, which is used by medical specialists to confirm pneumonia and other medical concerns, though they are not often the sole point of diagnosis. Different radiographic images taken at separate time intervals, such as before and during an illness, are often useful to physicians during the diagnosis. In general, these images form up an important part of an often multi-stage diagnosis process.

The dataset was used in a binary classification setting, with candidate data samples corresponding to either Normal or Pneumonia classes. The original Chest X-Ray dataset was directly used in this experiment, as well as 3 other versions generated by the addition of different perturbations to the images. These alternate, differentially-private datasets were generated by drawing random samples from the Laplacian Mechanism mentioned in (Dwork et al., 2006b) with $\mu = 0$ and varying levels of scale i.e. β .

These perturbations were added directly to the input image to create a noisy representation for subsequent training. These 4 datasets were used in different experiments to train the Resnet-18 model to convergence. To train the model on these images, some pre-processing steps were undertaken. Input images passed to the deep neural network were scaled to 256×256 pixels, and normalized to 1. Therefore, the function f defined in Section 2.1 is the identity function and the sensitivity Δf is 1.

The experiments are all carried out using Python 3.8.2 and PyTorch 1.4.0. We trained separate instances of the pre-trained Resnet-18 model on these 4 image datasets, over 120 epochs. The best models from these runs were saved and analyzed. The tradeoff in accuracy with these varying scales of perturbations in the images was examined. Best model accuracies on both the train and test set are included in Table 1, along with the learning curves over 120 epochs of training in Figure 1. A validation set was used to tweak and improve training performance over the whole set of training epochs, and was excluded from the figures for clarity.


Figure 1. Accuracy vs Training Epochs for Resnet-18

There are some interesting insights that emerge from the data included in Table 1 and Figure 1. These findings emphasize the intuition that accuracy clearly diminishes as scale of perturbation of the images is increased, represented by β . This relationship generalizes to the whole training process across all 120 epochs. Another interesting finding is the behavior of the training and test curves at different perturbation levels with respect to each other. The best trade-off between model bias and variance seems to be with a β value of 2, and the other perturbation levels also seem to exhibit better general training than that of the model trained on the original dataset, which demonstrates overfitting to the training data. This may highlight the potential for differential privacy methods in improving model generalization to unseen data, which may be useful under certain considerations.

While this approach of Local-DP serves the theoretical guarantee of Differential Privacy, we notice that it does not always provide the visual level of privacy one expects. Going through the perturbed set of training images, there are cases when the perturbed image looks exactly the same as the original image and in some other cases it becomes totally blurred out bringing into question the authenticity of the visual privacy being provided. In other cases Local-DP can also cause excessive disruption in the sensitive regions of the image which was critical for the task in hand (detecting pneumonia in our case). As you can see in Figure 2. (b) and (c) the perturbations can sometimes disrupt the sensitive regions of the chest which can cause the model to train poorly. On the other hand, Figure 2 (d) has been completely blurred out.

Conclusion And Future Directions

In this paper, we provided an empirical evaluation of a computationally tractable 18-Layer Resnet on a medically

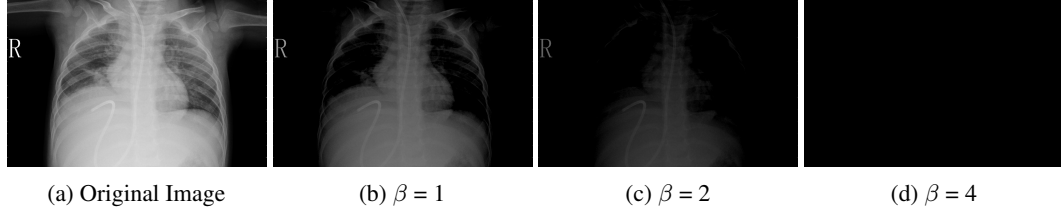


Figure 2. Comparison of sample image from dataset before and after Local DP based Obfuscation.

relevant classification task using the publicly available Chest X-Rays dataset. We observe that the Local-DP noise mechanisms leads to varied results with different perturbation levels and highlight the inherent trade-offs in these decisions. We also highlight interesting behavior in model performance on unseen data as a function of perturbation levels. This work also demonstrates the usefulness of transfer learning in privacy-preserving scenarios, as a pre-trained Resnet achieved good performance on another classification task across various perturbations.

We notice that while this form of Local-DP maintains the theoretical guarantee of Differential Privacy, it does not always provide the visual privacy we expect. On that end, we plan to continue this work to experiment with more privacy enhancing Local-DP techniques particularly one's which take into account the sensitive features (which are critical for model's training) to ensure that particular region does not get disrupted. Another derivative research direction we intend on pursuing is the effect of various perturbation levels on entire neural network topologies, such as those generated through meta learning methods (Elsken et al., 2018). Furthermore, different data modalities including audio files, video, text, tabular data, and various forms of cyber data can also be benchmarked in a similar way.

References

Covidview week 13. Technical report, Centers for Disease Control and Prevention(CDC), 2020.

Abadi, M., Chu, A., Goodfellow, I., McMahan, H. B., Mironov, I., Talwar, K., and Zhang, L. Deep learning with differential privacy. In *Proceedings of the 2016 ACM SIGSAC Conference on Computer and Communications Security*, pp. 308–318, 2016.

Bebensee, B. Local differential privacy: a tutorial. *arXiv preprint arXiv:1907.11908*, 2019.

Dwork, C., Kenthapadi, K., McSherry, F., Mironov, I., and Naor, M. Our data, ourselves: Privacy via distributed noise generation. In *Annual International Conference on the Theory and Applications of Cryptographic Techniques*, pp. 486–503. Springer, 2006a.

Dwork, C., McSherry, F., Nissim, K., and Smith, A. Calibrating noise to sensitivity in private data analysis. In *Theory of cryptography conference*, pp. 265–284. Springer, 2006b.

Dwork, C., Roth, A., et al. The algorithmic foundations of differential privacy. *Foundations and Trends® in Theoretical Computer Science*, 9(3–4):211–407, 2014.

Elsken, T., Metzen, J. H., and Hutter, F. Neural architecture search: A survey. *arXiv preprint arXiv:1808.05377*, 2018.

Fan, L. Differential privacy for image publication. 2019.

He, K., Zhang, X., Ren, S., and Sun, J. Deep residual learning for image recognition. In *Proceedings of the IEEE conference on computer vision and pattern recognition*, pp. 770–778, 2016.

Howley, E. K. What is coronavirus pneumonia? Technical report, US News and World Report, 2020.

Kermany, D. S., Goldbaum, M., Cai, W., Valentim, C. C., Liang, H., Baxter, S. L., McKeown, A., Yang, G., Wu, X., Yan, F., et al. Identifying medical diagnoses and treatable diseases by image-based deep learning. *Cell*, 172(5):1122–1131, 2018.

Miresghallah, F., Taram, M., Jalali, A., Elthakeb, A. T., Tullsen, D., and Esmaeilzadeh, H. A principled approach to learning stochastic representations for privacy in deep neural inference. *arXiv preprint arXiv:2003.12154*, 2020.

Miresghallah, F., Taram, M., Vepakomma, P., Singh, A., Raskar, R., and Esmaeilzadeh, H. Privacy in deep learning: A survey. *arXiv preprint arXiv:2004.12254*, 2020.

Simonyan, K. and Zisserman, A. Very deep convolutional networks for large-scale image recognition. *arXiv preprint arXiv:1409.1556*, 2014.

Szegedy, C., Ioffe, S., Vanhoucke, V., and Alemi, A. A. Inception-v4, inception-resnet and the impact of residual connections on learning. In *Thirty-first AAAI conference on artificial intelligence*, 2017.

Wang, J., Zhang, J., Bao, W., Zhu, X., Cao, B., and Yu, P. S. Not just privacy: Improving performance of private deep learning in mobile cloud. In *Proceedings of the 24th ACM SIGKDD International Conference on Knowledge Discovery & Data Mining*, pp. 2407–2416, 2018.